Investigation of selenization and various CBD CdS deposition conditions to fabricate high performing spray pyrolysis synthesized $Cu(In,Ga)(S,Se)_2$ solar cells

Muhammad Aamir Hassan,[1] Mohammad Mujahid,[1,a)] Shin Woei Leow,[2] Li WenJie,[2] Rajiv Ramanujam Prabhakar,[2] and Lydia Helena Wong[2,3]
[1]*School of Chemical and Materials Engineering, National University of Sciences and Technology, Sector H-12, Islamabad 44000, Pakistan*
[2]*Energy Research Institute @ NTU (ERI@N), Nanyang Technological University, Singapore*
[3]*School of Materials Science and Engineering, Nanyang Technological University, Singapore*

(Received 27 August 2016; accepted 25 January 2017; published online 14 February 2017)

Semiconducting thin-films of CIGS were deposited by spray pyrolysis of aqueous precursor solutions. The as-sprayed thin films were then selenized at different temperatures and durations to obtain the optimized selenization conditions (500 °C for 10 min). The chemical bath deposition process was used to deposit cadmium sulphide (CdS) using two different cadmium sources (cadmium acetate and cadmium sulphate) at various deposition times followed by post CdS annealing. Solar cells fabricated with CdS as the buffer layer using cadmium acetate show power conversion efficiency of 9.91% owing to its higher transmission and smaller grain size. *Published by AIP Publishing.* [http://dx.doi.org/10.1063/1.4976019]

I. INTRODUCTION

Chalcopyrite $Cu(In,Ga)(S,Se)_2$ (CIGSSe) is a promising light harvesting material and has been widely used in thin film solar cells because of its high optical absorption coefficient, modifiable band gap, long-term device stability, and high theoretical efficiency.[1–6] CIGS solar cells have obtained conversion efficiency of as high as 21.7%;[7,8] however, such a performance comes at the expense of high production cost with costly vacuum based deposition processes.[9,10] Solution-based fabrication of CIGS thin film based solar cells has the potential to cost lower with large scale roll to roll processing. Solution-based deposition of the CIGS films is generally performed using methods such as spin coating, spray-pyrolysis of precursor solutions onto the substrate, and doctor blading.[11–23] The as-deposited films are polycrystalline and require further annealing to promote grain growth to improve electrical properties, band gap, and absorption characteristics.[12] The selenization temperature profile is very important for the quality and performance of CIGSSe thin films, with the best technique producing large grain single phase chalcopyrite films.[24] After selenization, a buffer layer is deposited on the absorber layer. Even though the pn-junction is formed between p-type CIGS and n-type TCO layers, the quality of the junction and the performance of the device improve considerably with the introduction of the intermediate buffer layer. The band structure of the pn-junction is affected by the buffer layer, and hence, it affects the electric field, and thus, the current transport. The buffer layer also prevents shunting between the absorber and TCO layer because of its high resistance, passivates the CIGS surface defects, and protects the absorber layer from damage when the other layers are deposited on top of it.[25–27] The Cadmium sulphide (CdS) thin film deposited by the chemical bath deposition (CBD) method is used as a buffer layer in high efficiency solar cells based on CIGS and CdTe.[25] The CBD to deposit CdS thin film offers low cost per surface area of deposition, better morphological and photoconductivity properties, such as less roughness

[a)]Author to whom correspondence should be addressed. Electronic mail: mujahids@gmail.com

and pinhole density, in comparison to vacuum based methods for depositing CdS layer.[26,27] Cadmium acetate and cadmium sulphate are the two most commonly used Cd sources for CdS deposition.[12,17,24,26] The choice of the Cd source influences the electrical/optical properties, thickness, grain size, and surface morphology of CdS, and as a consequence, the quality of the CIGS/CdS junction is also influenced. The stability constants of Cd complexes and the deposition process, such as cluster by cluster deposition or ion by ion deposition, affect the properties of the CdS films.[28]

In this study, spray pyrolysis, as described in earlier works,[12–14] is employed to deposit CIGS using water as the solvent and non-toxic chemicals to avoid issues related to toxicity and carbonaceous impurities, which may arise especially when alcohols are used in the precursor solution.[12,29] The selenization processing conditions for CIGS thin films deposited by sputtering[24] and spin coating[11] were chosen initially for selenization of our spray-pyrolysis deposited CIGS samples, but the efficiencies of devices were very low; therefore, we optimized the selenization process for our spray-pyrolysis deposited CIGS devices. We deposited CdS buffer layer by chemical bath deposition using two different Cd sources (cadmium acetate and cadmium sulphate) while varying the deposition time, followed by studying the effect of annealing of CdS buffer layer. A CIGS thin film of our optimized conditions for selenization and CdS deposition with optimized composition[12] leads to a PCE of 9.91% measured on the cell area of 0.15 cm^2.

II. EXPERIMENTAL DETAILS

CIGS absorber layers were deposited by spray pyrolysis of aqueous precursor solutions of copper, indium, gallium, and sulphur sources onto commercially obtained molybdenum (Mo) coated soda-lime glass (SLG) substrate purchased from MTI Corporation. The solutions of 0.2 M gallium (III) chloride ($GaCl_3$, anhydrous 99.999% Sigma Aldrich), 1.0 M copper (II) chloride dehydrate ($CuCl_2.2H_2O$, 99.99% Sigma Aldrich), 0.2 M indium chloride ($InCl_3$, anhydrous 99.999% Sigma Aldrich), and 1.0 M thiourea (SC $(NH_2)_2$, 99.0% Sigma Aldrich) were prepared and used as stock solutions. The precursor solution containing Ga, In, Cu, S, and deionized (DI) water was sprayed onto Mo at the substrate temperature of 325 °C inside the fume hood with N_2 as carrier gas at a pressure of around 3 bars. At the temperature of 300 °C or more, the precursor material decomposes on the substrate, and the resulting thin film may contain impurity phases and it is amorphous or non-crystalline in nature.[14] In order for the grain growth and the densification of the films, the as-sprayed CIGS thin films were selenized in an argon filled single-zone selenization tube furnace (Thermo Scientific). After selenization, the CIGS films were transformed to $Cu(In,Ga)(S,Se)_2$ (CIGSSe). The selenized thin films were cooled to room temperature and then immediately transferred from the tube furnace into the chemical bath for depositing the thin layer of cadmium sulphide (CdS).

CdS buffer layers were deposited on as-selenized films using two different sets of precursors. The one set of precursors solutions to deposit CdS thin films contained deionized water, 0.015 M cadmium sulphate ($CdSO_4$, 99.0%, Sigma Aldrich), 0.75 M thiourea ($SC(NH_2)_2$, 99.0%, Sigma Aldrich), and ammonium hydroxide solution (NH_4OH, 28%–30% solution, Sigma Aldrich). The other set of precursors solutions contained deionized water, 0.25 M cadmium acetate dihydrate ($Cd(CH_3COO)_2{\cdot}2H_2O$, 98%, Sigma Aldrich), 0.75 M thiourea ($SC(NH_2)_2$, 99.0%, Sigma Aldrich), and ammonium hydroxide solution (NH_4OH, 28%–30% solution, Sigma Aldrich). The temperature of the water bath was maintained at 80 °C. Intrinsic ZnO (i-ZnO) and aluminium-doped ZnO (AZO) thin films of about 50 nm and 800 nm, respectively, were deposited using a Univex 350 sputtering system generating an RF power of 100 W for 10 min and DC power of 200 W for 35 min, respectively. Subsequently, they were mechanically scribed to define the active area of the individual solar cell to be 0.15 cm^2. In order to collect photo-generated charge carriers and reduce the series resistance, the silver glue was used to deposit top electrode in the form of a very thin line on the top of the individual solar cell.

The crystal structure of the films was determined by using the X-ray diffraction (XRD) method with a Bruker D8 Advance diffractometer with Cu $K\alpha_1$ radiation ($\lambda = 0.154056$ nm).

The microstructure of CIGSSe thin films was analysed with a Field-emission scanning electron microscope (FESEM, JEOL JSM-7600 F). Energy-dispersive X-ray spectroscopy (EDS) analyzer fitted with FESEM was used for the elemental analysis of the thin films. The absorption spectroscopy studies of the films were done by using UV-3600 Shimadzu UV-Vis-NIR spectrophotometer. In order to study the surface morphology of the films, the atomic force microscopy (AFM) was done with an Asylum Research Atomic Force Microscope.

The current-voltage characteristics of fabricated solar cells devices were measured using a solar simulator (VS-0852) under the simulated AM 1.5. 100 mW cm^{-2} illumination using a Keithley Source meter (2612A) and IV tester software package. The incident photon to current efficiency (IPCE) was measured using PVE300 photovoltaic device characterization system (Bentham).

III. RESULTS AND DISCUSSION

In order to obtain the optimized selenization conditions, solar cell devices were fabricated keeping all parameters constant except selenization conditions. The as-sprayed films were selenized at 480 °C for 10 min (sample A), 500 °C for 10 min (sample B), 530 °C for 10 min (sample C), and 500 °C for 30 min (sample D). The selenization temperature was increased from 480 °C to 530 °C for samples A to C while the selenization time was kept the same. The SEM image of sample A (Fig. 1(a)) revealed that the grain size was smaller compared to the other samples and the EDS analysis showed that the film contained more sulphur in comparison to selenium, suggesting incomplete selenization. It is suggested that sample A did not perform well because the selenization temperature was not enough for sufficient grain growth, densification, and selenium incorporation which led to poor electrical properties. Sample B performed better compared to the other samples (Table I), although the grain size was not as large as in sample C (Fig. 1(a)) but the film was dense and EDS analysis showed that the film contained similar Cu/(In + Ga) ratio as it was kept in the precursor solution (Table I) and it contained more selenium in comparison to sulphur, suggesting appropriate selenization. Although sample C had much better grain size compared to samples A and B (Fig. 1(a)), it was found from the EDS analysis that its Cu/(In + Ga) ratio dropped considerably (Table I). It is suggested that the drop in Cu/(In + Ga) ratio is due to the evaporation of the constituent elements of the films, which is responsible for the poor device performance because it can lead to the formation of secondary phases that are conducting in nature and can drastically affect the electrical properties of the films.[12] Sample D was selenized at the same temperature as sample B, but the selenization time for sample D was increased in order to improve the grain size to improve the electrical properties. The SEM image of sample D (Fig. 1(a)) showed that grain size was the largest among others, but EDS revealed that the film contained the least Cu/(In + Ga) ratio and its performance was worst compared to other samples (Table I). It is suggested that evaporation of constituent elements of the films is responsible for poor device performance. The as sprayed CIGS thin films and selenized thin films were characterized by using XRD (Fig. 1(b)). The

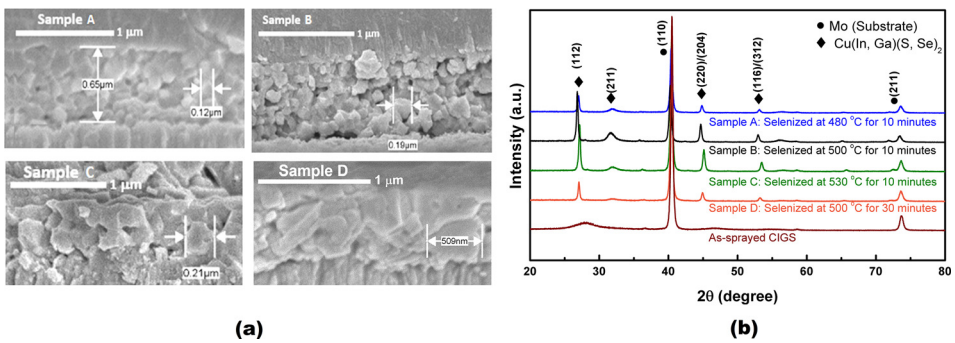

FIG. 1. CIGSSe solar cells fabricated using different selenization conditions. (a) Cross-section SEM images; (b) XRD patterns of constituent CIGSSe absorber films.

TABLE I. J-V characteristics of CIGSSe solar cells using different selenization conditions.

Sample No.	Sel. temp. (°C)	Sel. time (min)	$\frac{Cu}{In+Ga}$ (precursor solution)	$\frac{Cu}{In+Ga}$ (EDS)	V_{oc} (V)	j (mA/cm^2)	η (%)	FF (%)	R_{sh} (Ω cm^2)	R_s (Ω cm^2)
A	480	10	0.864	0.856	0.2537	15.081	1.326	34.659	174.20	12.12
B	500	10	0.864	0.849	0.4956	24.352	7.434	61.599	2762.07	8.36
C	530	10	0.864	0.676	0.2166	15.822	1.265	36.929	154.61	11.08
D	500	30	0.864	0.587	0.2053	8.757	0.709	39.440	291.38	10.82

XRD patterns reveal that as-sprayed films have poor crystallinity as their peaks have low intensities and broad, full width at half maximum (FWHM). The selenized films have narrower full width at half maximum (FWHM), indicating a significant increase in crystallinity. The XRD patterns are left-shifted for selenized films, indicating that the lattice expansion of CIGSSe films is due to the incorporation of Se during selenization. The XRD peaks for samples A, B, C, and D are marginally shifted with respect to each other. It is suggested that the S/Se ratio in the samples is slightly different because of different annealing times and temperatures, consequently causing a minor shift in the XRD peaks. It was concluded that the optimized selenization temperature for CIGSSe thin films deposited by spray pyrolysis is 500 °C for 10 min because the films had decent grain size, densification, and selenium incorporation, which led to better electrical properties, and hence, the device performed superior compared to other devices.

After obtaining the optimized conditions for selenization, solar cell devices were fabricated keeping all parameters constant, except the CBD CdS deposition conditions. The optimum thickness of CdS buffer layer is around 50–60 nm.[7,30] A thicker buffer layer would lead to a decrease in the number of photons absorbed by the CIGS layer.[30] Different deposition times were explored to deposit the CdS films of optimum thickness, obtained from $CdSO_4$ and $Cd(CH_3COO)_2{\cdot}2H_2O$. The thickness of the films was measured by AFM imaging by masking half of the sample using tape; hence, there was a region without CdS and a region with CdS, and so, we probed the AFM on the boundary to measure the thickness of the CdS. The dependence of the film thickness on deposition time is listed in Table II. The film thickness increased with the deposition time, irrespective of the Cd source used, but the growth of CdS using $CdSO_4$ was faster compared to the growth of CdS using $Cd(CH_3COO)_2{\cdot}2H_2O$ because of the smaller stability constant of $Cd[SO_4]_3^{-4}$ complex.[28,31] UV-VIS spectroscopy and surface roughness measurement by the software from AFM images revealed that CdS films (thickness around 55 nm) obtained from $Cd(CH_3COO)_2{\cdot}2H_2O$ have a higher transmittance and smaller grain size (around 70 nm) compared to CdS films (thickness around 50 nm and grain size around 130 nm) obtained from the $CdSO_4$ (Figs. 2 and 3). It has been reported that the growth rate of CdS using $CdSO_4$ is faster compared to the other Cd sources, and hence, the resultant grain size is larger.[28,32] It is suggested that the CdS film obtained from $Cd(CH_3COO)_2{\cdot}2H_2O$ have higher transmittance owing to the smaller grain size of CdS. The as-deposited CdS films were

TABLE II. Dependence of film thickness on deposition time and grain size dependence on two different Cd sources.

Cd source	Average grain size (nm)	Deposition time (min)	Film thickness (nm)
$Cd(CH_3COO)_2{\cdot}2H_2O$	70	9	35
		11	55
		13	70
$CdSO_4$	130	6	30
		8	50
		10	65

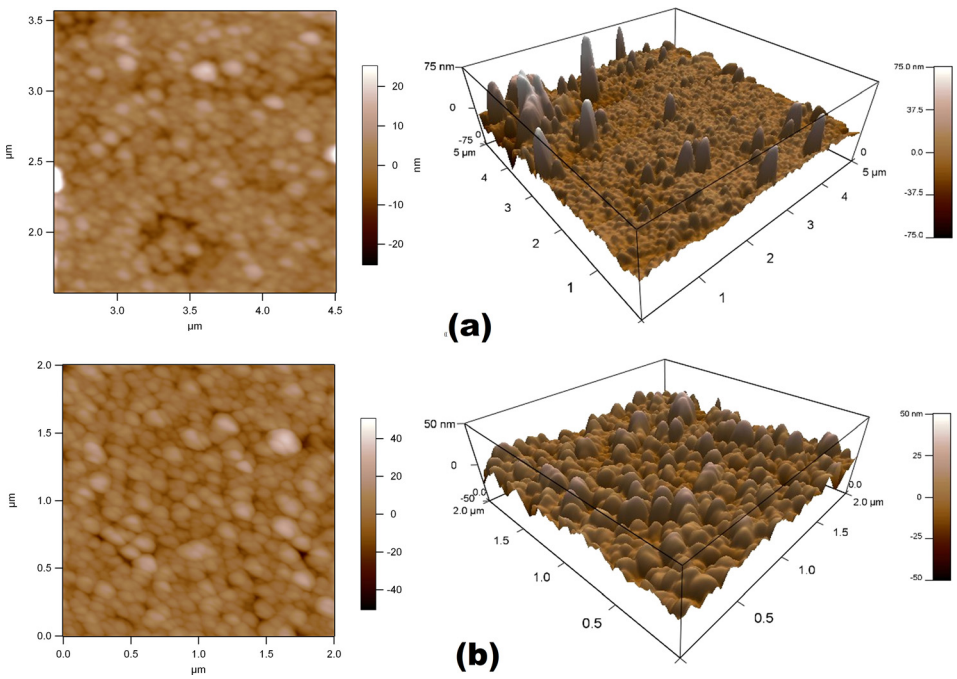

FIG. 2. (a) 2D and 3D AFM surface morphology images of CdS deposited using $CdSO_4$ precursor; (b) 2D and 3D AFM surface morphology images of CdS deposited using $Cd(CH_3COO)_2{\cdot}2H_2O$ precursor.

annealed for 2 min at the substrate temperature of 200 °C in open air. UV-VIS spectroscopy revealed that annealing of the CdS thin films slightly decreases their transmittance (Fig. 3). It is suggested that annealing helps in improving the crystallinity of CdS and hence decreases the transmittance. The performance of the solar cell devices fabricated with CdS buffer layers deposited using various deposition conditions is listed in Table III. The thicker CdS films helped in improving the V_{oc} by improving the junction quality, but j_{sc} decreased significantly because the thicker CdS limits the number of photons reaching the absorber (Fig. 4(c)). The thinner CdS films helped in improving the j_{sc} by allowing more photons to reach the absorber, but V_{oc} was lower because of poor junction quality (Fig. 4(c)). The post CdS annealing of the films helped in gaining V_{oc} by improving the CdS-CIGSSe interface as annealing helps the CdS to slightly diffuse into the CIGSSe absorber; thus, the devices with annealed CdS

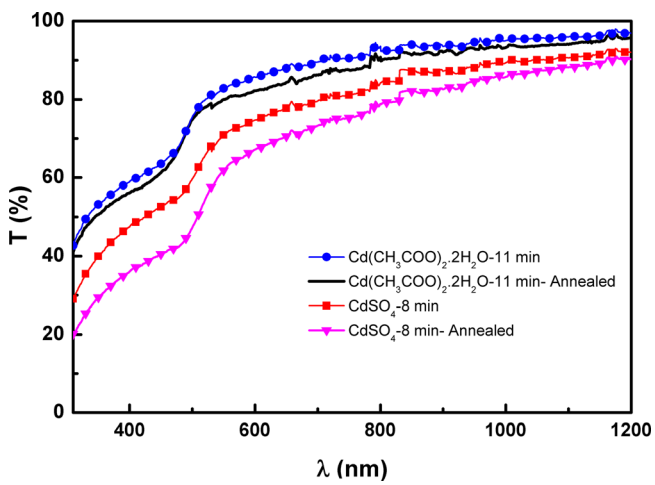

FIG. 3. UV-Vis-NIR transmission spectra of CdS thin films deposited on glass.

TABLE III. J-V characteristics of CIGSSe solar cells containing CdS buffer layers of various thicknesses deposited using $CdSO_4$ and $Cd(CH_3COO)_2{\cdot}2H_2O$ precursors.

Sample No.	Precursor	Dep. time (min)	Post CdS annealing (2 min at 200 °C)	V_{oc} (V)	j (mA/cm^2)	η (%)	FF (%)	R_{sh} (Ω cm^2)	R_s (Ω cm^2)
1	$Cd(CH_3COO)_2$	9	No	0.4861	23.0649	6.39	57.03	1497.13	10.35
			Yes	0.4870	23.7559	6.56	56.71	1521.81	9.19
2	$Cd(CH_3COO)_2$	11	No	0.5812	23.4014	9.46	69.53	2265.10	10.03
			Yes	0.5882	23.3307	9.91	72.21	2440.75	8.81
3	$Cd(CH_3COO)_2$	13	No	0.6119	17.1332	7.16	68.31	3495.85	28.45
			Yes	0.6171	17.5467	7.56	69.79	3401.84	28.31
4	$CdSO_4$	6	No	0.4445	22.7785	5.21	51.47	1977.43	9.52
			Yes	0.4407	22.6094	5.13	51.52	1931.53	9.22
5	$CdSO_4$	8	No	0.5808	19.6113	6.84	60.01	2356.38	21.19
			Yes	0.5799	19.5340	6.81	60.11	2297.67	22.78
6	$CdSO_4$	10	No	0.6122	15.8359	6.66	68.69	3664.05	35.03
			Yes	0.6095	16.9284	6.88	66.70	3560.06	36.23

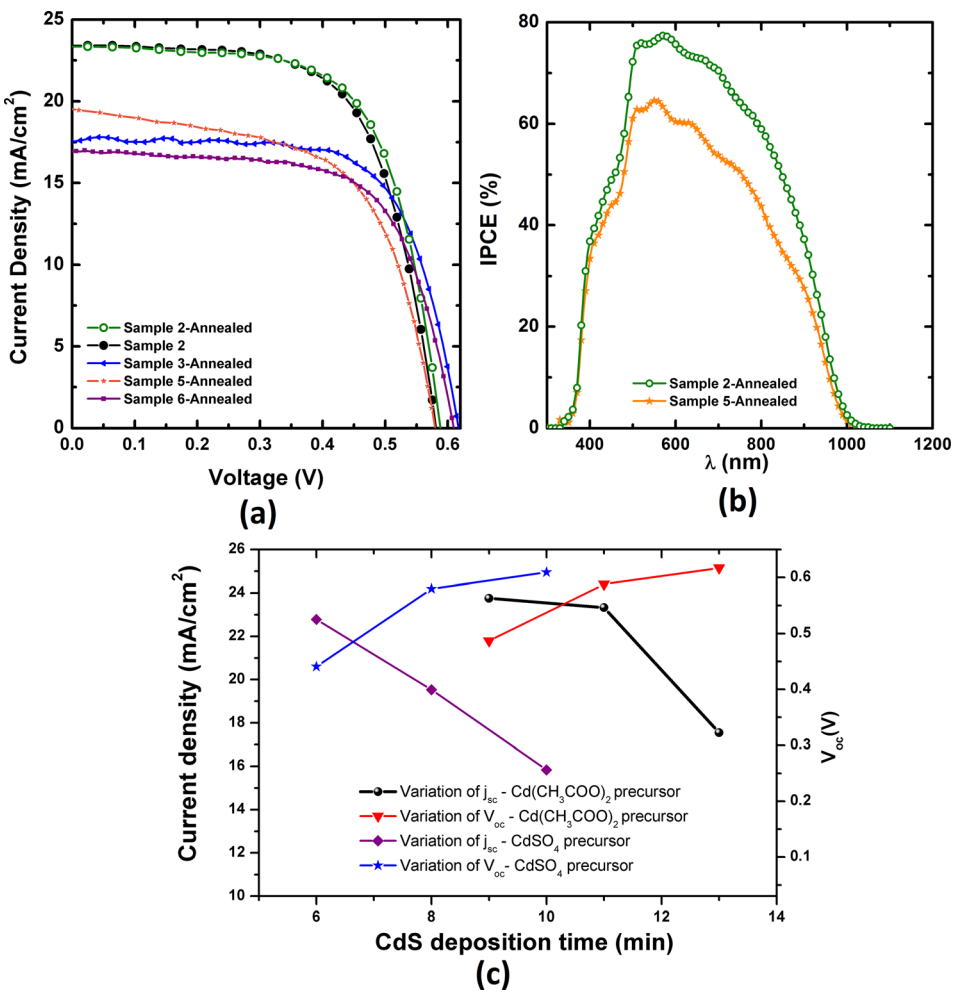

FIG. 4. (a) j-V curves of devices fabricated using the CdS buffer layer of various thicknesses deposited using $CdSO_4$ and $Cd(CH_3COO)_2{\cdot}2H_2O$ precursors. (b) The IPCE spectra of sample 2 and sample 5 and (c) V_{oc} and j_{sc} variation with CdS deposition time.

performed slightly better (Table III, Fig. 4(a)), as reported earlier.[33,34] Samples 2 and 5 performed the best among the devices containing the CdS obtained from $Cd(CH_3COO)_2{\cdot}2H_2O$ and $CdSO_4$, respectively (Table III). The peak IPCE drops for sample 5 compared to sample 2 (Fig. 4(b)), which is in agreement with the results from UV-VIS spectroscopy (Fig. 3). The device containing the CdS buffer layer deposited using $Cd(CH_3COO)_2{\cdot}2H_2O$ precursor for 11 min and then annealed at 200 °C in open air had the highest efficiency compared to other devices (Figs. 4(a) and 4(b) and Table III). The CdS buffer layer deposited using $Cd(CH_3COO)_2{\cdot}2H_2O$ had smaller grain size and higher transmission compared to CdS deposited using $CdSO_4$. It is suggested that the small grain size of CdS helped in forming a very good conformal CdS layer on CIGSSe film, and higher transmission of CdS allows more photons to reach the absorber CIGSSe thin film. The annealing also helped in improving the device efficiency slightly.

IV. CONCLUSIONS

The spray-pyrolysis method was used to deposit thin films of $Cu(In,Ga)(S,Se)_2$ onto Mo-coated soda-lime glass using water based precursors. The selenization temperature of 500 °C for 10 min was found to be optimum for our CIGSSe thin film solar cells. The chemical bath deposition of CdS using $Cd(CH_3COO)_2{\cdot}2H_2O$ precursors performs better because of higher transmission and smaller grain size compared to CdS thin film deposited using $CdSO_4$ precursor. The optimum thickness of CdS should be around 50–60 nm (the thickness below this will affect the V_{oc} and higher than this will drastically reduce the j_{sc}).

ACKNOWLEDGMENTS

The research work would not have been possible without the collaboration and research support provided by the Energy Research Institute (ERI@N) and School of Materials Science and Engineering at Nanyang Technological University Singapore.

[1]H. Zhou, C.-J. Hsu, W.-C. Hsu, H.-S. Duan, C.-H. Chung, W. Yang, and Y. Yang, Adv. Energy Mater. **3**(3), 328–336 (2013).
[2]B. Bob, B. Lei, C.-H. Chung, W. Yang, W.-C. Hsu, H.-S. Duan, W. W.-J. Hou, S.-H. Li, and Y. Yang, Adv. Energy Mater. **2**(5), 504–522 (2012).
[3]N. G. Dhere, Sol. Energy Mater. Sol. Cells **91**(15–16), 1376–1382 (2007).
[4]X.-J. Wu, X. Huang, X. Qi, H. Li, B. Li, and H. Zhang, Angew. Chem. Int. Ed. Engl. **53**(34), 8929–8933 (2014).
[5]Q. Guo, S. J. Kim, M. Kar, W. N. Shafarman, R. W. Birkmire, E. A. Stach, R. Agrawal, and H. W. Hillhouse, Nano Lett. **8**(9), 2982–2987 (2008).
[6]Q. Guo, G. M. Ford, H. W. Hillhouse, and R. Agrawal, Nano Lett. **9**(8), 3060–3065 (2009).
[7]P. Jackson, D. Hariskos, R. Wuerz, O. Kiowski, A. Bauer, T. M. Friedlmeier, and M. Powalla, Phys. Status Solidi RRL **9**(1), 28–31 (2015).
[8]M. A. Green, K. Emery, Y. Hishikawa, W. Warta, and E. D. Dunlop, Prog. Photovoltaics: Res. Appl. **23**(7), 805–812 (2015).
[9]I. Repins, M. A. Contreras, B. Egaas, C. DeHart, J. Scharf, C. L. Perkins, B. To, and R. Noufi, Prog. Photovoltaics: Res. Appl. **16**(3), 235–239 (2008).
[10]A. Chirilă, P. Reinhard, F. Pianezzi, P. Bloesch, A. R. Uhl, C. Fella, L. Kranz, D. Keller, C. Gretener, H. Hagendorfer, D. Jaeger, R. Erni, S. Nishiwaki, S. Buecheler, and A. N. Tiwari, Nat. Mater. **12**(12), 1107–1111 (2013).
[11]W. Wang, S.-Y. Han, S.-J. Sung, D.-H. Kim, and C.-H. Chang, Phys. Chem. Chem. Phys. **14**(31), 11154–11159 (2012).
[12]M. A. Hossain, Z. Tianliang, L. K. Keat, L. Xianglin, R. R. Prabhakar, S. K. Batabyal, S. G. Mhaisalkar, and L. H. Wong, J. Mater. Chem. A **3**(8), 4147–4154 (2015).
[13]Y. Cai, J. C. W. Ho, S. K. Batabyal, W. Liu, Y. Sun, S. G. Mhaisalkar, and L. H. Wong, ACS Appl. Mater. Interfaces **5**(5), 1533–1537 (2013).
[14]J. C. W. Ho, T. Zhang, K. K. Lee, S. K. Batabyal, A. I. Y. Tok, and L. H. Wong, ACS Appl. Mater. Interfaces **6**(9), 6638–6643 (2014).
[15]W. Liu, D. B. Mitzi, M. Yuan, A. J. Kellock, S. J. Chey, and O. Gunawan, Chem. Mater. **22**(3), 1010–1014 (2010).
[16]S. J. Park, J. W. Cho, J. K. Lee, K. Shin, J.-H. Kim, and B. K. Min, Prog. Photovoltaics: Res. Appl. **22**(1), 122–128 (2014).
[17]V. A. Akhavan, T. B. Harvey, C. J. Stolle, D. P. Ostrowski, M. S. Glaz, B. W. Goodfellow, M. G. Panthani, D. K. Reid, D. A. Vanden Bout, and B. A. Korgel, ChemSusChem **6**(3), 481–486 (2013).
[18]T. K. Todorov, O. Gunawan, T. Gokmen, and D. B. Mitzi, Prog. Photovoltaics: Res. Appl. **21**(1), 82–87 (2013).
[19]S. Ahn, K. Kim, A. Cho, J. Gwak, J. H. Yun, K. Shin, S. Ahn, and K. Yoon, ACS Appl. Mater. Interfaces **4**(3), 1530–1536 (2012).
[20]S. M. McLeod, C. J. Hages, N. J. Carter, and R. Agrawal, Prog. Photovoltaics: Res. Appl. **23**(11), 1550–1556 (2015).
[21]A. R. Uhl, J. K. Katahara, and H. W. Hillhouse, Energy Environ. Sci. **9**(1), 130–134 (2016).
[22]U. Berner and M. Widenmeyer, Prog. Photovoltaics: Res. Appl. **23**(10), 1260–1266 (2015).

[23]W. Zhao, Y. Cui, and D. Pan, Energy Technol. **1**(2–3), 131–134 (2013).
[24]W. Li, Y. Sun, W. Liu, and L. Zhou, Sol. Energy **80**(2), 191–195 (2006).
[25]J. Britt and C. Ferekides, Appl. Phys. Lett. **62**(22), 2851–2852 (1993).
[26]H. R. Moutinho, D. Albin, Y. Yan, R. G. Dhere, X. Li, C. Perkins, C. S. Jiang, B. To, and M. M. Al-Jassim, Thin Solid Films **436**(2), 175–180 (2003).
[27]R. Mendoza-Pérez, G. Santana-Rodríguez, J. Sastre-Hernández, A. Morales-Acevedo, A. Arias-Carbajal, O. Vigil-Galan, J. C. Alonso, and G. Contreras-Puente, Thin Solid Films **480–481**, 173–176 (2005).
[28]H. Khallaf, I. O. Oladeji, G. Chai, and L. Chow, Thin Solid Films **516**(21), 7306–7312 (2008).
[29]A. R. Uhl, C. Fella, A. Chirilă, M. R. Kaelin, L. Karvonen, A. Weidenkaff, C. N. Borca, D. Grolimund, Y. E. Romanyuk, and A. N. Tiwari, Prog. Photovoltaics: Res. Appl. **20**(5), 526–533 (2012).
[30]P. Chelvanathan, M. I. Hossain, and N. Amin, Curr. Appl. Phys. **10**(Suppl. 3), S387–S391 (2010).
[31]L. G. Sillén, A. E. Martell, and J. Bjerrum, *Stability Constants of Metal-Ion Complexes* (Chemical Society, London, 1964).
[32]I. Kaur, D. K. Pandya, and K. L. Chopra, J. Electrochem. Soc. **127**(4), 943–948 (1980).
[33]Y.-D. Chung, D.-H. Cho, N.-M. Park, K.-S. Lee, and J. Kim, Curr. Appl. Phys. **11**(Suppl. 1), S65–S67 (2011).
[34]T. Sakurai, N. Ishida, S. Ishizuka, M. M. Islam, A. Kasai, K. Matsubara, K. Sakurai, A. Yamada, K. Akimoto, and S. Niki, Thin Solid Films **516**(20), 7036–7040 (2008).